

1 Biobased pH-responsive and self-healing hydrogels prepared from O-carboxymethyl chitosan  
2 and a 3-dimensional dynamer as cartilage engineering scaffold  
3

4 Rui Yu,<sup>a</sup> Yan Zhang,<sup>d</sup> Mihail Barboiu,<sup>a\*</sup> Marie Maumus,<sup>b</sup> Danièle Noël,<sup>b,c\*</sup> Christian  
5 Jorgensen,<sup>b,c</sup> Suming Li<sup>a\*</sup>  
6

7 <sup>a</sup> *Institut Européen des Membranes, IEM UMR 5635, Univ Montpellier, CNRS, ENSCM,*  
8 *Montpellier, France*

9 <sup>b</sup> *IRMB, Univ Montpellier, INSERM, Montpellier, France;*

10 <sup>c</sup> *Clinical Immunology and Osteoarticular Diseases Therapeutic Unit, Hôpital Lapeyronie,*  
11 *Montpellier, France*

12 <sup>d</sup> *Key Laboratory of Carbohydrate Chemistry and Biotechnology, Ministry of Education, School*  
13 *of Pharmaceutical Sciences, Jiangnan University, 1800 Lihu Avenue, Wuxi, 214122, China*  
14

15 \* Corresponding authors: [suming.li@umontpellier.fr](mailto:suming.li@umontpellier.fr) (S. Li)

16 [mihail-dumitru.barboiu@umontpellier.fr](mailto:mihail-dumitru.barboiu@umontpellier.fr) (M. Barboiu), and [daniele.noel@inserm.fr](mailto:daniele.noel@inserm.fr) (D. Noel)

## Abstract:

Novel dynamic hydrogels were prepared from O-carboxymethyl chitosan (CMCS) and a water soluble dynamer Dy via crosslinking by imine bond formation using an environmentally friendly method. Dy was synthesized by reaction of Benzene-1,3,5-tricarbaldehyde with Jeffamine. The resulting soft hydrogels exhibit a porous and interconnected morphology, storage modulus up to 1400 Pa, and excellent pH-sensitive swelling properties. The swelling ratio is relatively low at acidic pH due to electrostatic attraction, and becomes exceptionally high up to 7000% at pH 8 due to electrostatic repulsion. Moreover, hydrogels present outstanding self-healing properties as evidenced by closure of split pieces and rheological measurements. This study opens up a new horizon in the preparation of dynamic hydrogels with great potential for applications in drug delivery, wound dressing, and in particular in tissue engineering as the hydrogels present excellent cytocompatibility.

Keywords: O-carboxymethyl chitosan; Imine chemistry; Dynamic hydrogel; Self-healing; pH responsive; Cytocompatibility

## 1. Introduction

In the past decades, hydrogels have been widely studied as biomaterials for various applications in drug delivery, wound dressing and tissue engineering due to their outstanding properties such as biocompatibility (Qu et al., 2018), biodegradability (Ghobril & Grinstaff, 2015), mechanical properties (Van Vlierberghe, Dubruel, & Schacht, 2011), and stimuli-responsive properties (Zhang, Tao, Li, & Wei, 2011). Hydrogels consist of a cross-linked network (Lv et al., 2018; Su et al., 2015) which can absorb large amounts of water (Yang, Wang,

Yang, Wang, & Wu, 2018) or physiological fluids (Dimatteo, Darling, & Segura, 2018) while maintaining their three-dimensional structural integrity. Hydrogels can be classified into two categories according to the preparation approach: chemical gels or irreversible gels, and physical gels or reversible gels (Iftime, Morariu, & Marin, 2017; Stewart et al., 2017). Chemical gels are formed by irreversible covalent bonding, whereas in physical gels, the polymeric chains are held together by chain entanglements and/or supramolecular hydrophobic, ion-pair or hydrogen bonding interactions.

Dynamic hydrogels or dynagels are a dynamic system on both the molecular and supramolecular levels (Burdick & Murphy, 2012; Marin et al., 2014). They are able to reversibly exchange their components (Sreenivasachary & Lehn, 2005), responding to external stimuli such as pH (Zeng et al., 2017), ions (Arnal Hérault, Banu, Barboiu, Michau, & van der Lee, 2007; Rotaru et al., 2017), and temperature (Zhang, Jin, Li, Zhang, & Wu, 2018). Among the various dynamic reactions (Zhang & Barboiu, 2015a), imine bond formation is considered as the most promising strategy to generate dynamic materials with modifiable properties. In fact, imine chemistry allows to implement reversible rearrangements of the components in a multivalent material which can bind bioactive molecules, cells or present self-healing properties (Chao, Negulescu, & Zhang, 2016). This dynamic constitutional framework is composed of linear and/or multi-armed components reversibly interconnected via imine bonds and containing stimuli-responsive functional groups (Zhang & Barboiu, 2015b).

Chitosan (CS), a polysaccharide obtained from alkaline hydrolysis of chitin found in the exoskeleton of crustaceans, presents remarkable properties such as biocompatibility, biodegradability, low toxicity, low cost or immune-stimulatory activity (Ali & Ahmed, 2018). Chitosan is a good candidate for in-situ dynamic reversible crosslinking via its amino groups

present along the polymer chain with aldehydes (Marin, Simionescu, & Barboiu, 2012), alginate (Qin et al., 2019), or gelatin (Qiao, Ma, Zhang, & Yao, 2017), resulting in the formation of pH-responsive and biodegradable hydrogels. The water solubility of chitosan depends on many factors, in particular pH of the medium, chain length and degree of acetylation (Varum, Ottoy, & Smidsrod, 1994). The carboxymethylation of the D-glucosamine moieties of chitosan generates O-carboxymethyl chitosan (CMCS) which is readily soluble in water at neutral pH, thus allowing uses in tissue engineering, drug delivery, wound dressing and food industry.

Crosslinking of CS or CMCS with aldehydes via imine bond formation along polymeric chains proceeds with very low yield in aqueous medium, but is significantly improved in hydrogels or in solid state films with dynamic properties (Marin et al., 2012). It is well known that no continuous cross-linked networks are formed when monoaldehydes (Iftime et al., 2017; Marin, et al., 2012) or dialdehydes (Yu et al., 2017) are used for cross-linking. The resulting hydrogels exhibit good swelling behaviors, but disordered micro-structure and weak mechanical strength. In contrast, dynamic hydrogels exhibiting pH and temperature-responsive swelling behaviors, strong mechanical performance, and self-healing behavior have been obtained by using 3-armed (Deng et al., 2015) or 4-armed aldehydes (Huang et al., 2016). Nevertheless, the toxicity of aldehydes, and especially of glutaraldehyde (Bhatia, 2010; Ghobril & Grinstaff, 2015) restricts their use for biomedical applications, and imposes the necessity of finding new biocompatible crosslinking agents.

Jeffamine is a polyetheramine composed of poly(propylene oxide) (PPO) and/or poly(ethylene oxide) (PEO) blocks with primary amino groups attached to the chain ends. It is widely used as a macromonomer to prepare PEO-based hydrogels as its water solubility facilitates reaction in aqueous medium (Zimmermann, Bittner, Stark, & Mülhaupt, 2002). In this work, bifunctional

Jeffamine ED-2003 was linked to benzene-1,3,5-tricarbaldehyde via imine formation, yielding a constitutional dynamer Dy that can be used as a water soluble cross-linking component. CMCS based hydrogels were then prepared by mixing CMCS and Dy aqueous solutions through a “green” synthetic route. The chemical structures of the hydrogels, their morphological, rheological and swelling properties, as well as their self-healing behaviors were evaluated and discussed. The cytocompatibility of hydrogels was assessed by co-culture in the presence of human mesenchymal stromal cells (MSCs) to evaluate their potential as scaffold in cartilage engineering.

## 2. Experimental section

2.1 Materials: Benzene-1,3,5-tricarbaldehyde (BTA) from Manchester Organics and O,O'-Bis(2-aminopropyl) PPO-*b*-PEO-*b*-PPO (Jeffamine<sup>®</sup> ED-2003,  $M_n 1.9 \times 10^3$ ) from Sigma Aldrich were used without purification. CMCS ( $M_n 2 \times 10^5$  Da, degree of deacetylation 90 %, degree of carboxymethylation 80 %) was purchased from Golden-shell Biochemical Co., Ltd. Methanol (96%), citric acid ( $\geq 99.5\%$ ), disodium hydrogen phosphate dodecahydrate ( $\geq 99\%$ ), boric acid ( $\geq 99.5\%$ ), borax ( $\geq 99\%$ ) were of analytical grade, and obtained from Sigma Aldrich.

2.2 Synthesis of dynamer Dy: Typically, BTA (162 mg, 1 mmol), Jeffamine (1.90 g, 1 mmol) are added in 30 mL methanol, and the reaction mixture was stirred at 70 °C for 4 h. After evaporation of the solvent, 20 mL Milli Q water was added, yielding a homogeneous dynamer solution of  $5 \times 10^{-2}$  M as calculated from the remaining aldehyde groups.

2.3 Preparation of CMCS-Dy hydrogels: CMCS (1.06 g, 5 mmol calculated from D-glucosamine units) was dissolved in 50 mL Milli-Q water at room temperature, yielding a transparent solution of  $1 \times 10^{-1}$  M. CMCS and dynamer solutions were mixed at different ratios to a total volume of

12 mL, followed by ultra-sonication for 1 min to remove trapped bubbles. Gelation then proceeded at 37 °C for 24 h, yielding a CMCS-based hydrogel.

Freeze-drying was performed as follows so as to conserve the original structure. As-prepared hydrogels were placed in small vials and immersed in liquid nitrogen (-196 °C) for instantaneous freezing. The vials were then placed in a 500 mL round-bottomed flask which was fixed on LABCONCO® freeze dryer. The hydrogels were freeze-dried for 24 h before analyses.

2.4 Characterization: <sup>1</sup>H NMR spectroscopy was carried out using Bruker NMR spectrometer (AMX500) of 300 MHz. CDCl<sub>3</sub> or D<sub>2</sub>O was used as the solvent. 5 mg of sample were dissolved in 0.5 mL of solvent for each analysis. Chemical shifts were recorded in ppm using tetramethylsilane (TMS) as internal reference. The morphology of freeze dried hydrogels was examined using scanning electron microscopy (SEM, Hitachi S4800). The samples were subjected to gold coating prior to analysis. Fourier-transform infrared spectroscopy (FT-IR) was performed with Nicolet Nexus FT-IR spectrometer, equipped with ATR diamant Golden Gate.

2.5 Structural stability of Dy: The stability of the dynamer Dy was evaluated in D<sub>2</sub>O under neutral and acidic conditions since imine bond formation is reversible at low pH. D<sub>2</sub>O solutions at pH of 1, 3, and 5 were prepared by addition of trifluoroacetic acid. NMR spectra were registered just after dynamer dissolution and after 7 days.

2.6 Rheology: The rheological properties of hydrogels were examined with Physical MCR 301 Rheometer (Anton Paar). Hydrogels prepared in Milli-Q water were placed on a cone plate (diameter of 4 cm, apex angle of 2 °, and clearance 56 µm). Measurements were made in the linear visco-elastic range as a function of time, strain, or frequency.

2.7 Swelling: The swelling behavior of hydrogels was evaluated in buffer solutions at various pH values. Solutions from pH 1 to pH 7 were prepared using 0.1 × 10<sup>-3</sup> M citric acid solution and

0.2 × 10<sup>-3</sup> M disodium hydrogen phosphate solution, whereas solutions of pH 8 and 9 were prepared using 0.2 × 10<sup>-3</sup> M boric acid solution and 0.5 × 10<sup>-4</sup> M borax solution. Freeze-dried gels were immersed in a buffer, and taken out at different time intervals. The swollen hydrogels were weighed after wiping surface water with filter paper, freeze-dried for 24 h, and weighed again. The swelling ratio and mass loss ratio of hydrogel were calculated according to equation (1) and equation (2), respectively:

$$\text{Swelling ratio \%} = \frac{(M_s - M_d)}{M_d} \times 100 \quad (1)$$

$$\text{Loss ratio \%} = \frac{(M_0 - M_d)}{M_0} \times 100 \quad (2)$$

Where M<sub>0</sub> is the initial mass of xerogel, M<sub>s</sub> is the wet mass of the swollen hydrogel, and M<sub>d</sub> is the dried mass of the swollen hydrogel after lyophilization.

2.8 Self-healing experiments: Various hydrogel samples were prepared in Milli-Q water, and in pH = 7 and pH = 8 buffers. Some of them were dyed yellow with 5 μL of lucigenin, or dyed red with Rhodamine. 3 different approaches were applied to examine the self-healing behavior of hydrogels: 1) a hole with diameter around 3 mm was punched at the circle center of the sample; 2) samples were split into two pieces, and then a yellow piece was put together with a transparent piece immediately at 37 °C ; 3) injection of transparent and red samples on the surface of a Petri dish to observe color changes.

2.9 Cell cultures and Cytotoxicity: 2 mL of CMCS at 100 mmol and 1 mL of dynamer at 50 mmol were mixed. Human MSCs isolated from adipose tissue (AT-MSCs) or from bone marrow (BM-MSCs) were added at a concentration of 1 × 10<sup>6</sup> cells / mL. As control, AT-MSCs or BM-MSCs were seeded on 96-wells TCPS (Tissue Culture Polystyrene System) plates at 5 × 10<sup>3</sup> cells per well, or were embedded in 3 mg / mL rat collagen type I hydrogel (Corning) at 1 × 10<sup>6</sup> cells / mL. 50 μL of cell laden solution were loaded in each well of 96 wells ultra-low adhesion plates

(Corning). After 2 h gelation in an atmosphere at 37 °C, 5 % CO<sub>2</sub> and 95 % of humidity, 100 µL of proliferative medium (αMEM containing 10% fetal calf serum, 100 µg/mL penicillin/streptomycin, 2 × 10<sup>-3</sup> M glutamine, 1 ng / mL of basic fibroblast growth factor) were added on the top of the hydrogel. MSCs were cultured for 7 days with medium change at day 3. After 1 or 7 days culture, the cell viability was analyzed by confocal microscopy (Leica) after staining the live cells in green and the dead cells in red using the live/dead assay kit (Invitrogen).

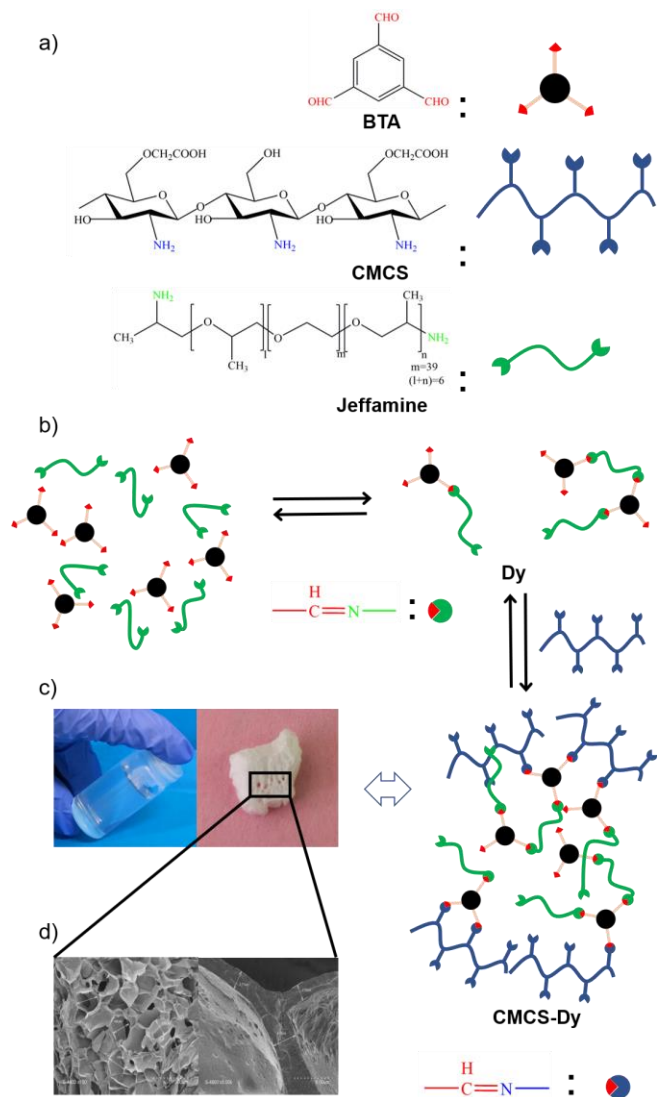
### 3. Results and discussion

3.1 Synthesis of dynamer: A water soluble dynamer Dy was first synthesized by reaction of BTA as the core structure and bifunctional diamine, Jeffamine<sup>®</sup> ED-2003 (Mn=1900) as the water-soluble linker at a molar ratio of 1:1 via reversible imine bond formation, as shown in Scheme 1. Thus, it remains in average one aldehyde group per molecule of BTA for further cross-linking reaction with the amine groups of CMCS.

<sup>1</sup>H NMR spectroscopy was used to monitor the formation and stability of imine bonds during the synthesis of the dynamer. Fig. 1 presents the <sup>1</sup>H NMR spectrum of the dynamer mixture obtained after 4 h reaction at 70 °C. Three signals of aldehyde groups are observed in the 10.1-10.3 ppm range, corresponding to different degrees of substitution in trialdehyde. Signals **a** at 10.21 ppm, **b** at 10.15 ppm, and **c** at 10.09 ppm belong to non-substituted, mono-substituted, and di-substituted trialdehydes, respectively. The molar ratio of signals **a**, **b** and **c** is 1:6.6:11.5, as determined from the peak integrations. These findings indicate formation of a dynamer with various free aldehyde groups, which is beneficial for subsequent crosslinking with amino groups of CMCS by imine formation. Signal **d** in the range of 8.0-8.7 ppm is assigned to the imine and aromatic protons, signal **e** around 3.7 ppm to the methylene and methine protons, and signal **f** around 1.2 ppm to



the methyl protons of Jeffamine, respectively (Catana et al., 2015). The presence of residual  $\text{CHCl}_3$  and  $\text{H}_2\text{O}$  is detected at 7.3 and 1.8 ppm, respectively.



**Scheme 1.** Synthesis route of CMCS-based dynamic hydrogel: a) chemical structures of BTA, CMCS and Jeffamine; b) synthesis of the dyanmer Dy by reaction of equimolar BTA and Jeffamine, and synthesis of hydrogel by imine formation between Dy and CMCS; c) images of as prepared hydrogel and freeze dried hydrogel; and d) SEM images of freeze dried hydrogel.

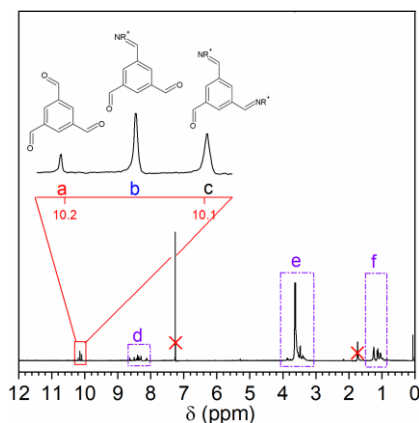


**Fig. 1.**  $^1\text{H}$  NMR spectrum of the dynamer Dy obtained by reaction of BTA and Jeffamine in  $\text{CDCl}_3$ .

The effect of reaction time on the formation of dynamer was investigated. No difference was observed on the  $^1\text{H}$  NMR spectra of samples up to 72 h reaction (Fig. S1, Supporting Information), thus implying that equilibrium was reached after 4 h reaction. Therefore, the dynamer obtained after 4 h reaction was selected for further studies. Moreover, the dynamer apparently remained unchanged for a week in pure  $\text{D}_2\text{O}$  and in acidic  $\text{D}_2\text{O}$  at pH 3 and 5, while became highly hydrolyzed in strongly acidic medium at pH 1 (Fig. 2). The spectra obtained in  $\text{D}_2\text{O}$  and at pH 3 and 5 remain unchanged even after 7 days (Fig. S2, Supporting Information). In contrast, major changes are observed on the spectrum of dynamer at pH 1. The signal **a** (10.21 ppm) belonging to free aldehydes becomes much more intense, indicating that imine bonds are hydrolyzed back to aldehydes. Therefore, the dynamer Dy seems stable at neutral and slightly acidic pH, but unstable at strongly acidic pH. As previously observed for PEGylated networks, Jeffamine chains could have a protecting effect against the hydrolysis of imine bonds, favoring the imine formation in slightly acidic or neutral media (Catana et al., 2015).

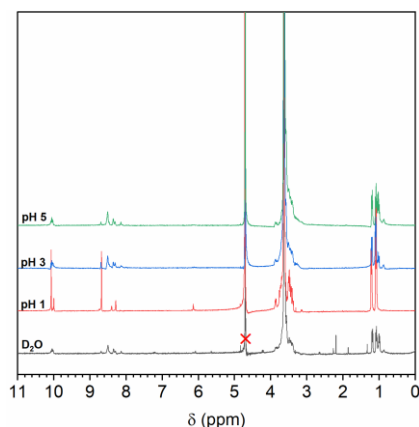


**Fig. 2.**  $^1\text{H}$  NMR spectra of the dynamer Dy in pure  $\text{D}_2\text{O}$  and acidic  $\text{D}_2\text{O}$  at  $\text{pH} = 1, 3$ , and  $5$

3.2 Synthesis of CMCS-Dy hydrogels: CMCS based hydrogels were prepared via a ‘green’ and environmentally friendly method, as shown in Scheme 1. The free aldehyde groups of Dy react with the amine groups of CMCS to form imine bonds in water, leading to a three-dimensional network of CMCS based hydrogel. A series of hydrogels were obtained by mixing  $1 \times 10^{-1}$  M CMCS and  $5 \times 10^{-2}$  M dynamer aqueous solutions to a total volume of 12 mL. Gelation proceeded at  $37^\circ\text{C}$  for 24 h. The D-glucosamine to dynamer molar ratio varied from 1:1 to 8:1, as shown in Table 1.

**Table 1.** Molar and mass composition of CMCS-Dy hydrogels <sup>a)</sup>

Sample	D-glucosamine/Dy molar ratio	CMCS <sup>b)</sup>			Dy			Total polymer concentration [w/v %]
		[mmol]	[mg]	[w/v %]	[mmol] <sup>c)</sup>	[mg] <sup>d)</sup>	[w/v %]	
Gel1-1	1:1	0.4	85	0.7	0.4	810	6.8	7.5
Gel2-1	2:1	0.6	127	1.1	0.3	608	5.0	6.1
Gel4-1	4:1	0.8	170	1.4	0.2	405	3.4	4.8
Gel6-1	6:1	0.9	191	1.6	0.15	304	2.5	4.1
Gel8-1	8:1	0.96	204	1.7	0.12	243	2.0	3.7

- a) Hydrogels are prepared by mixing CMCS and dynamer solutions at different ratios to a total volume of 12 mL;
- b) The concentration of CMCS solution is 100 mM. Calculations are made on the basis of the average molar mass of 212 g/mol obtained for D-glucosamine, taking into account the degree of deacetylation of 90 % and the degree of carboxymethylation of 80 %;
- c) The concentration of Dy solution is 50 mM calculated from the remaining aldehyde groups. In a typical reaction, 1 mmol BTA (162 mg) reacts with 1 mmol Jeffamine (1900 mg) to form a dynamer. As BTA has 3 aldehydes and Jeffamine 2 amines, there remains theoretically 1 mmol of aldehydes in the dried dynamer. Addition of 20 mL water yields a dynamer solution of 50 mM.
- d) The amount of Dy in solution is obtained from the initial quantities of BTA and Jeffamine.

FTIR was used to confirm the formation of imine bonds during the synthesis of the dynamer Dy and CMCS based hydrogel. As shown in Fig. 3, the characteristic bands of aldehyde and imine bonds are observed at 1698 and 1645  $\text{cm}^{-1}$  on the spectra of Dy, respectively. The dried gels present all the characteristic bands of CMCS and dynamer: a large band in the 3200-3500  $\text{cm}^{-1}$  assigned to free OH and  $\text{NH}_2$  groups, an intense band at 1595  $\text{cm}^{-1}$  assigned to carboxyl groups of CMCS, and two strong signals at 2850 and 1100  $\text{cm}^{-1}$  attributed to C-H and C-O stretching in the dynamer, respectively. With increasing D-glucosamine to dynamer molar ratio, the aldehyde band progressively disappears at ratios above 4:1, while the imine band merges with that of carboxyl groups at 1595  $\text{cm}^{-1}$  which turns more intense. These findings confirm that hydrogels are formed because of imine formation between aldehyde and amine groups.

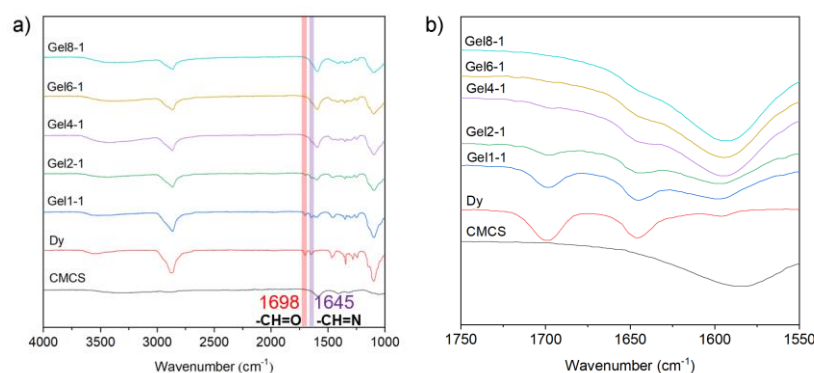


**Fig. 3.** a) FT-IR spectra and b) enlarged view of the 1550-1750  $\text{cm}^{-1}$  wavelength range of CMCS, dynamer Dy and freeze-dried CMCS-Dy hydrogels.

3.3 Rheological studies. The rheological properties of hydrogels were investigated under various conditions. CMCS and Dy aqueous solutions were mixed in situ on the plate of rheometer, and changes of the storage modulus ( $G'$ ) and loss modulus ( $G''$ ) were followed as a function of time at 37°C (Fig. 4a). For all samples, at the beginning of experiment the storage modulus is lower than the loss modulus ( $G' < G''$ ), which illustrates a liquid-like behavior of the starting mixture. After an induction time, both  $G'$  and  $G''$  begin to increase,  $G'$  increasing faster than  $G''$ . A crossover point between  $G'$  and  $G''$  is detected, indicating sol-gel transition. As shown in Figure 4a, the gelation time decreases from 600 s for Gel1-1 to a minimum of 360 s for Gel4-1, and then increases to 660 s for Gel8-1. In fact, gelation occurs by crosslinking via imine bonds formation and is thus dependent on the ratio between amine groups of CMCS and aldehyde groups of the dynamer. In Gel1-1, there are less amine groups than aldehyde ones, as calculated by taking into account the degree of deacetylation of 90 %. Thus, gelation is relatively slow. Gelation is progressively improved for Gel2-1 and Gel4-1, as the concentration of amine groups increases. Gelation is not optimal for Gel2-1, since unreacted aldehyde groups are detected by FTIR after 24 h at 37 °C (Fig. 3). In contrast, optimal imine bond formation is achieved for Gel4-1 as aldehyde groups are no longer detectable. Nevertheless, with further increase of D-glucosamine/dynamer ratio to 6:1 and 8:1, the gelation becomes longer as there are less aldehyde groups available for imine formation.

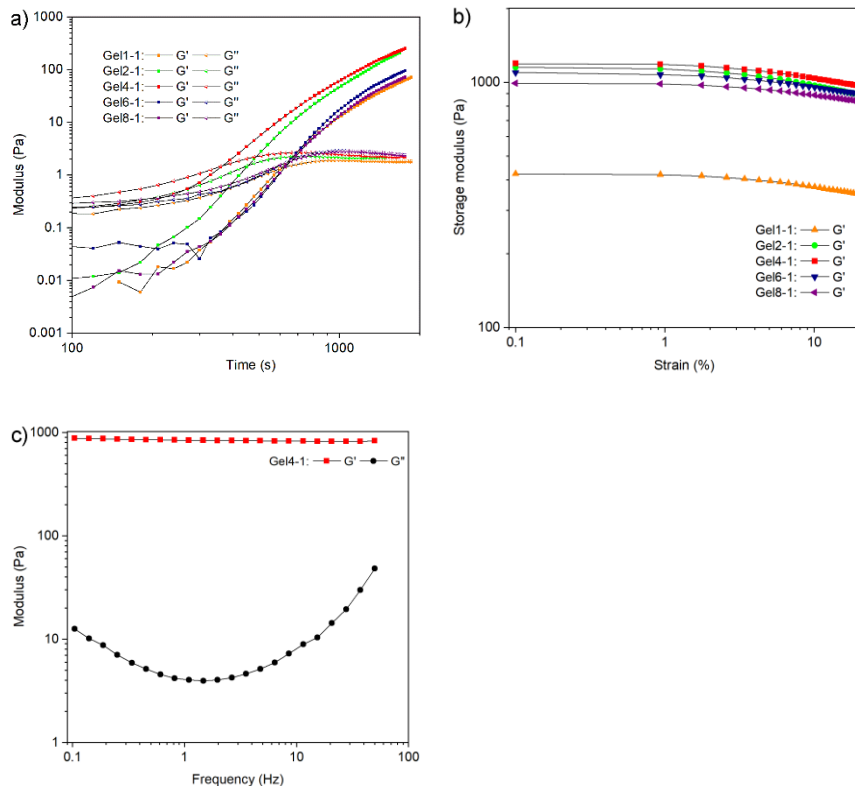


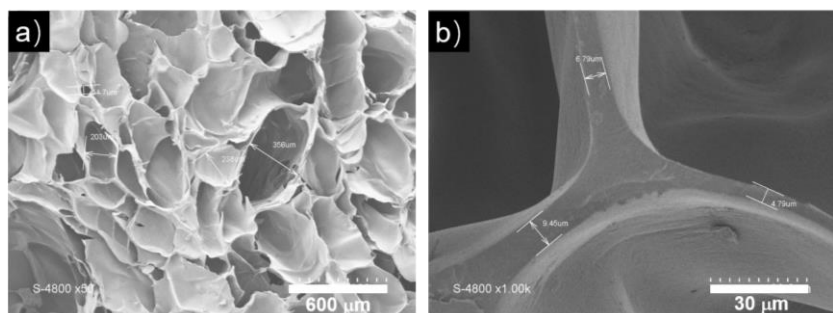
**Fig. 4.** a) Storage modulus ( $G'$ ) and loss modulus ( $G''$ ) changes as a function of time after mixing CMCS and Dy aqueous solutions at various ratios at 37 °C, strain of 1%, and frequency of 1 Hz; b)  $G'$  changes as a function of applied strain for all hydrogels at 25 °C, and frequency of 1 Hz; and c)  $G'$  and  $G''$  changes of Gel4-1 as a function of frequency at 25 °C, and strain of 1%. All hydrogels are prepared in Milli-Q water.

Rheological measurements performed at 25 °C illustrate the viscoelastic behaviors of as prepared hydrogels. The storage modulus of all gels slightly decreases (less than 20 % of the initial value) when increasing the strain up to 20 % (Fig. 4b), indicating that the hydrogels are stable in this strain range with viscoelastic behavior. On the other hand, the modulus increases with increasing D-glucosamine to dynamer molar ratio from 1:1 to 4:1, reaching a maximum value of *c.a.* 1200 Pa at 4:1. In contrast, higher D-glucosamine to dynamer ratios of 6:1 and 8:1 result in decrease in

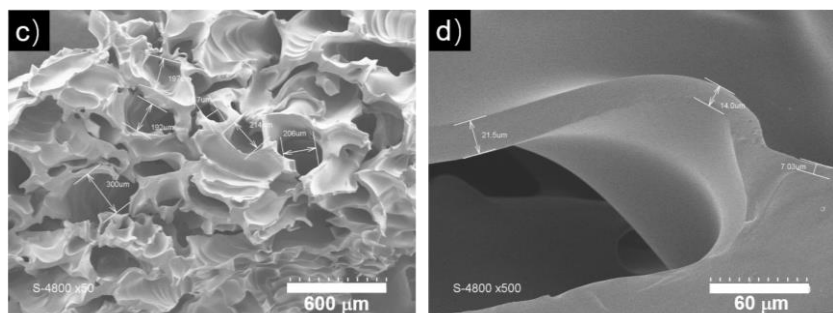
modulus because there are less aldehydes available for crosslinking in Gel6-1 and Gel8-1 compared to Gel4-1. These findings well agree with storage modulus ( $G'$ ) and loss modulus ( $G''$ ) changes versus time in Fig. 4a, confirming that optimal crosslinking is achieved with Gel4-1. In order to investigate the stability of the hydrogels, a frequency sweep over a range from 0.01 to 50 Hz was carried out at a fixed strain of 1 %. Taking Gel4-1 as an example (Fig. 4c), the storage modulus  $G'$  is always much higher than the loss modulus  $G''$ .  $G'$  remains nearly unchanged, whereas  $G''$  exhibits some fluctuations with increasing frequency. The other hydrogels exhibit similar behaviors (Fig. S3, Supporting Information). These rheological results well corroborate with the formation of highly stable covalent networks, in contrast to physical hydrogels whose storage and loss moduli are dependent on the frequency (Li, El Ghzaoui, & Dewinck, 2005; Zhang et al., 2010). It is generally admitted that hydrogels with  $G'$  below 2000 Pa are 'soft' materials suitable for specific tissue engineering applications (brain, cartilage, muscle, etc).

3.4 Morphology and swelling studies: Scanning electron microscopy (SEM) was used to qualitatively assess the microstructure of the freeze-dried hydrogels. As shown in Fig. 5, all samples exhibit a sponge-like structure with open and interconnected pores. Gel4-1 apparently exhibits the most uniform porous structure with mean pore size around 150  $\mu\text{m}$  and mean wall thickness of *c.a* 3  $\mu\text{m}$ , whereas the other samples, in particular Gel1-1 and Gel8-1, present larger and irregular pore size and larger wall thickness. These findings well agree with the optimal imine formation or crosslinking of Gel4-1 since higher crosslinking leads to smaller pore size and wall thickness.

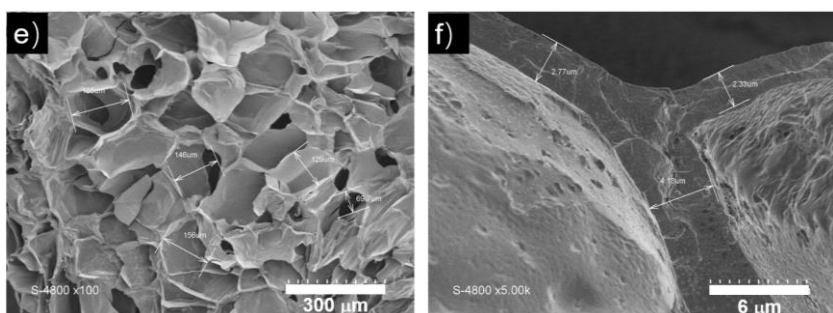
297



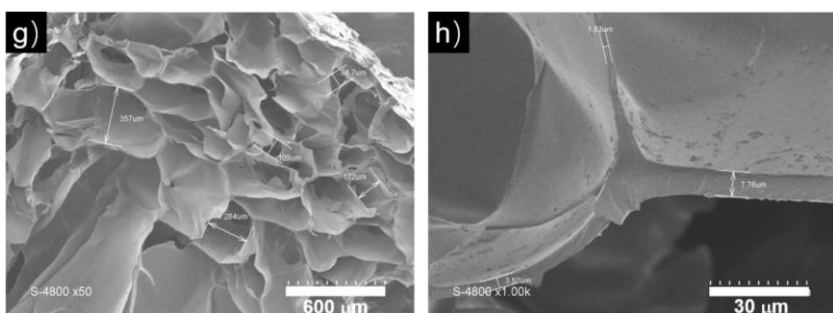
298



299



300



301

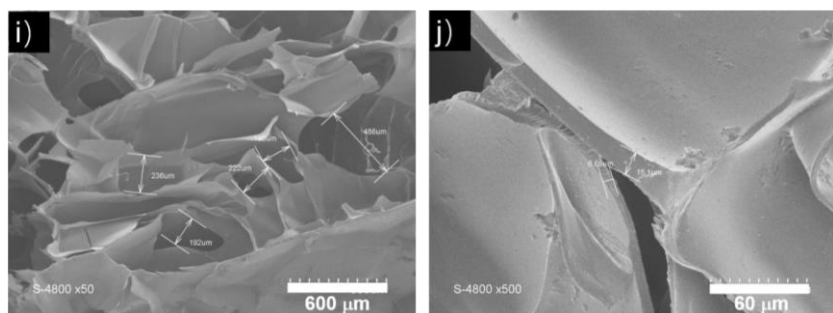


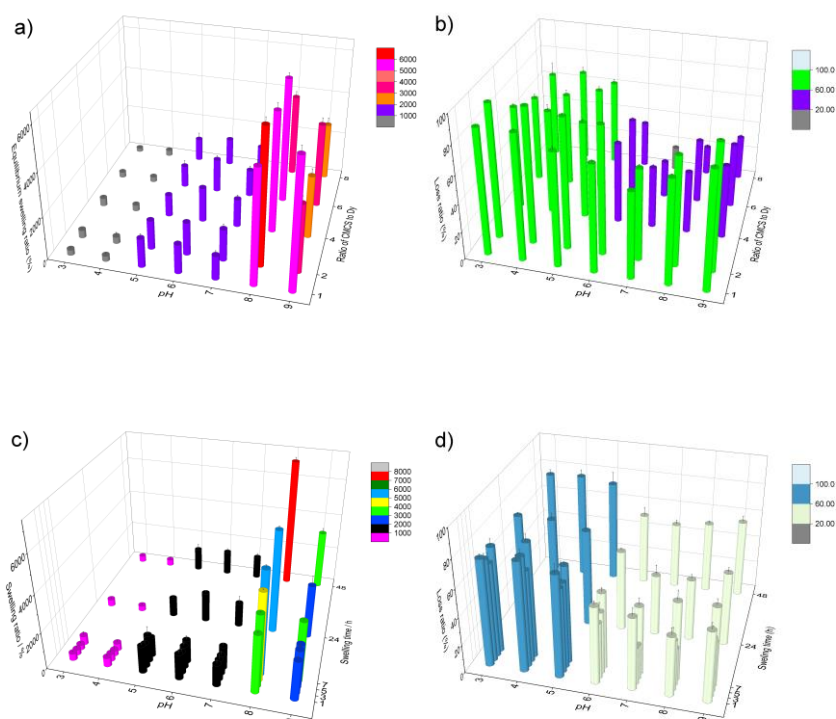


**Fig. 5.** SEM images of freeze dried hydrogels: (a, b) Gel1-1; (c, d) Gel2-1; (e, f) Gel4-1; (g, h) Gel6-1; (i, j) Gel8-1.

The swelling behaviors of hydrogels are of major importance for the applications as drug carrier or as tissue engineering scaffold. The five samples exhibit similar swelling behaviors at a given pH value in the pH range from 3 to 9. The highly pH-sensitive swelling ratios are below 1000 % for acidic media (gray bar, pH 3/4), between 1000 % and 2000 % for neutral media (violet bar, pH 5/6/7), above 2000 % and up to 6000 % for alkaline media (orange bar, pink bar, reddish orange bar, magenta bar, and red bar, pH 8/9) as shown in Fig. 6a. Interestingly, when immersed in slightly alkaline medium at pH 8, the swelling ratio of Gel4-1 dramatically depends on the immersion time (Fig. 6c). It increases from 3130 % (green bar) after 1 h to 7050 % (red bar) after 48 h immersion. In more alkaline medium at pH 9, the variation of the swelling ratio is attenuated, from 2500 % (blue bar) after 1 h to 3500 % (green bar) after 48 h immersion (Fig. 6c). In contrast, this exceptional time dependent swelling behavior of Gel4-1 rapidly reaches an equilibrium at 1 h for pH 3-7.

Mass loss could occur after swelling of hydrogels at various pH values, resulting from the diffusion and washing away of non-crosslinked species, including those initially present or formed by hydrolysis of imine bonds under acidic conditions. Thus the mass loss ratio reflects the crosslinking degree and the stability of hydrogels. Obviously, when immersed in acidic media at  $\text{pH} \leq 5$  for all hydrogels or in the whole pH range for Gel1-1 and Gel2-1 with low CMCS and high Dy contents (Fig. 6b), the mass loss ratio is above 60 % (green bar). Loss ratios below 60 % (violet and gray bars) are obtained only in neutral or alkaline media ( $\text{pH} \geq 6$ ) for Gel4-1 with optimal crosslinking, and Gel6-1 and Gel8-1 with decreasing Dy content (Table 1).

These findings indicate that higher Dy content and acidic medium are conducive to the mass loss of hydrogels during swelling. It is thus supposed that unconnected or incompletely connected Dy is predominant in the soluble fraction. Dy rings or homopolymers could be formed during reaction of BTA and Jeffamine (Scheme 1). These species may escape coupling with CMCS in the hydrogel preparation procedure. This assumption is consistent with IR analysis showing the presence of the aldehyde band for Gel1-1 and Gel2-1, and its absence for Gel4-1, Gel6-1 and Gel8-1 samples (Fig. 3). The reaction conditions could be improved by reducing the time and/or lowering the temperature to minimize the formation of these species.



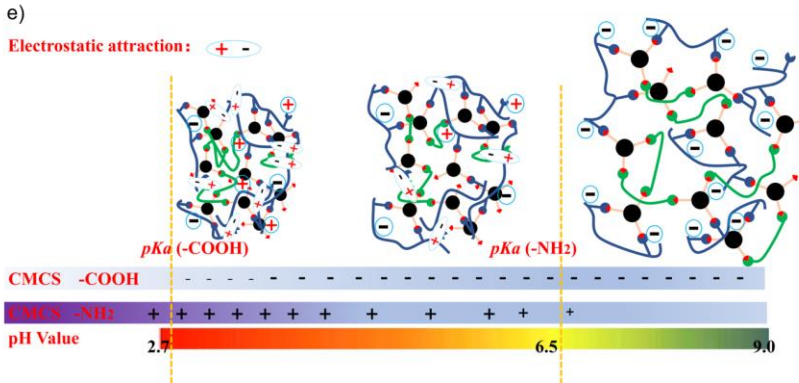


**Fig. 6.** a) Equilibrium swelling ratios, and b) Mass loss ratios of Gel1-1, Gel2-1, Gel4-1, Gel6-1, and Gel8-1 at various pH values for 24 h, c) Swelling ratios, and d) Mass loss ratios of Gel4-1 at different pH values as a function of immersion time, e) Schematic presentation of the swelling behavior of freeze-dried hydrogels immersed in buffers at various pH values.

The mass loss ratio of Gel4-1 also varies with immersion time at different pH values: in the range of 20-60 % (milk white bar) up to 48 h in neutral / alkaline media at  $pH \geq 6$ , and above 60% (dusty blue bar) in acidic media at  $pH=3-5$  probably because of the partial hydrolysis of imine bonds (Fig. 6d). These results indicate that freeze dried hydrogels could be interesting for uses in physiological environment owing to higher swelling and better stability.

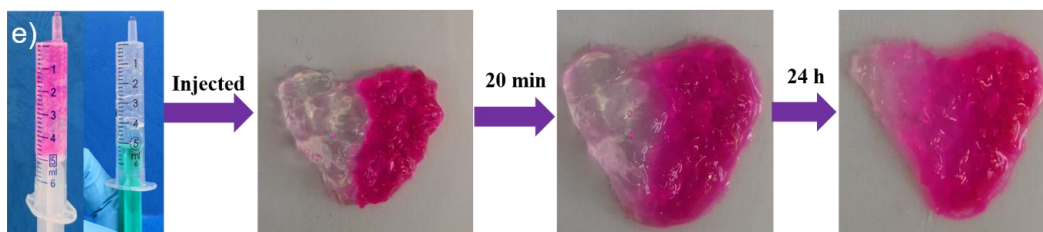
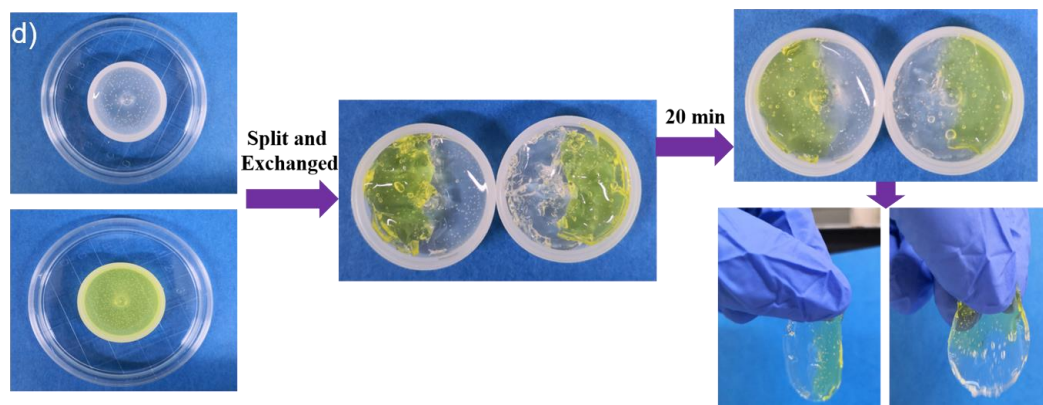
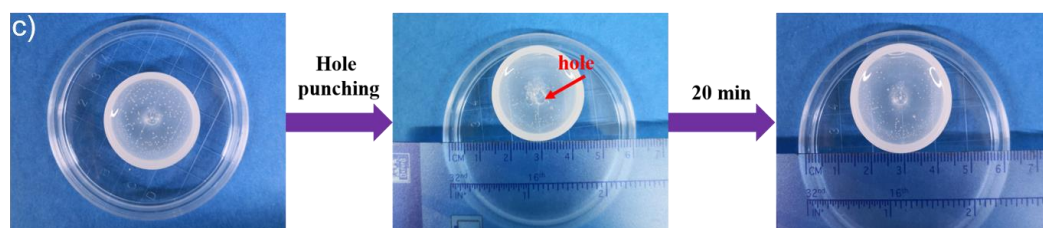
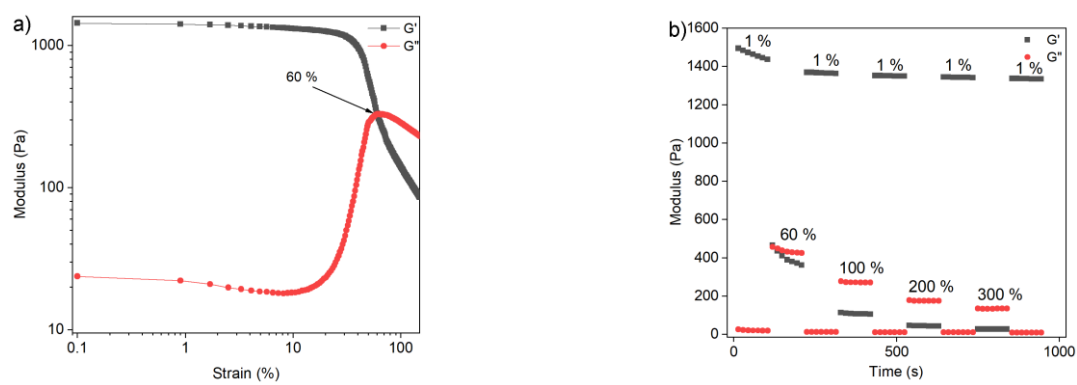
The pH dependent swelling behaviors of hydrogels could be explained by the electrostatic interactions due to the presence of amino and carboxyl groups along CMCS chains. In fact, the  $pK_a$  of amino and carboxyl groups is 6.5 and 2.7 (Lv et al., 2018), respectively. Thus, at acidic pH 3 and 4, there is strong electrostatic attraction between negatively charged  $-COO^-$  and positively charged  $-NH_3^+$  groups, which results in shrinkage or low swelling ratio of hydrogels (Fig. 6e). With increasing pH up to 7, there are less protonated  $NH_3^+$  and ionized  $-COO^-$  groups, leading to lower electrostatic attraction and higher swelling. In contrast, at pH 8, the  $NH_2$  groups are not charged, while the electrostatic repulsion between the charged  $-COO^-$  groups along

CMCS chains leads to strong swelling. However, at pH 9, the electrostatic repulsion between the  $\text{-COO}^-$  groups is counterbalanced by the  $\text{OH}^-$  ions in solution. Consequently, the swelling is attenuated as compared to that observed at pH 8.

Changes of the micro-structure of hydrogels were observed by using SEM after 24 h swelling at two pH values. At pH 4, all freeze-dried hydrogels strongly shrink with reduced pore size and pore number (Fig. S4, Supporting Information). Noticeably, the pore size of Gel4-1 decreases from *c.a* 150 to 100  $\mu\text{m}$ , and the wall thickness increases from *c.a* 3.5  $\mu\text{m}$  to 15  $\mu\text{m}$ , reminiscent with the contraction of hydrogels due to electrostatic attraction at acidic pH (Figure 6e). In contrast, expansion of the porous structure is observed at pH 8 (Fig. S5, Supporting Information). The pores wall shows a cracked structure, with the thickness strongly decreasing from *c.a* 3.5  $\mu\text{m}$  to 200-600 nm due to strong swelling of hydrogels provoked by electrostatic repulsion at basic pH (Fig. 6e).

**3.5 Self-healing:** CMCS-based hydrogels present interesting self-healing behaviors as evidenced by rheological recovery tests at fixed frequency of 1 Hz and at 37°C. Gel4-1 hydrogels were prepared in Milli-Q water, and in pH 7 and pH 8 buffers in order to examine the self-healing behavior under different swollen conditions. Gelation was realized at 37°C for 24 h. As shown in Fig. 7a, both the storage modulus ( $G'$ ) and loss modulus ( $G''$ ) of Gel4-1 in Milli-Q water slightly decreases until a strain of 20%. Beyond,  $G'$  dramatically decreases, whereas  $G''$  rapidly increases. A crossover point of  $G'$  and  $G''$  values is observed at a strain of 60%. Similar profiles are observed for Gel4-1 at pH 7 with a crossover point at 35% (Fig. S6a, Supporting Information). In contrast, Gel4-1 at pH 8 exhibits lower storage modulus because of its highly swollen state as

shown in Figure 6a. A crossover point of  $G'$  and  $G''$  is detected at 55% at pH 8 (Fig. S6c, Supporting Information).



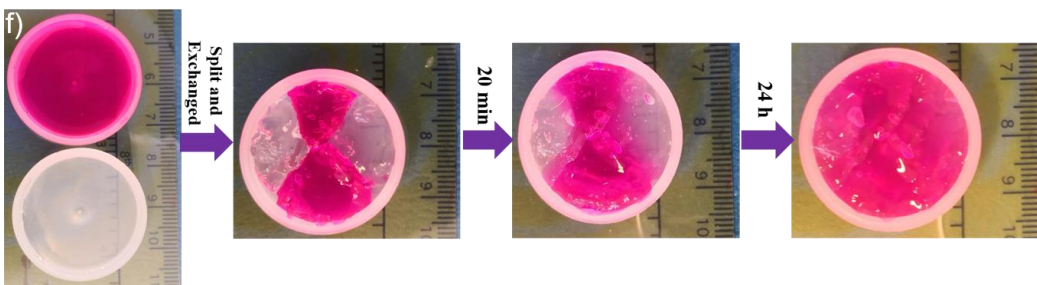


**Fig. 7.** a) Modulus changes as a function of strain of Gel4-1 prepared in Milli-Q water; b) Modulus changes of Gel4-1 prepared in Milli-Q water with alternatively applied high and low oscillatory shear strains at 37°C; c-f) Self-healing macroscopic approaches using hydrogel samples prepared in Milli-Q water (c-d), at pH 7 (e) and at pH 8 (f) , see text for details.

Based on the strain amplitude sweep results, continuous step strain measurements were performed to examine the rheological recovery behavior of Gel4-1. At 1 %, Gel4-1 in Milli-Q water behaves as a hydrogel since  $G'$  is largely superior to  $G''$ . As the oscillatory shear strain increases from 1% to 60% and is maintained at 60% for 105 s (Fig. 7b),  $G'$  becomes lower than  $G''$ , indicating the destruction of hydrogel structure. Both  $G'$  and  $G''$  immediately recover their initial values when the strain is back to 1%. Modulus recovery is observed when larger strains (100, 200, and 300%) and small strain (1%) are alternatively applied. Similar phenomena are also observed for Gel4-1 prepared in pH 7 and 8 buffers (Fig. S6b, S6d, Supporting Information). Therefore, it could be concluded that dynamic hydrogels exhibit rapid recovery (self-healing) behavior probably due to the reconstruction of reversible imine bond linkage when they are subjected to alternatively applied high and low oscillatory shear strains.

The self-healing behavior of Gel4-1 was further evidenced with four different macroscopic approaches using one transparent hydrogel sample and another one incorporating yellow lucigenin or red Rhodamine B dyes. First, a hole with diameter of 3 mm was punched at the

center of a hydrogel sample prepared in Milli-Q water, and the hole disappeared after 20 min at 37°C (Fig. 7c). In a second approach, transparent and yellow hydrogel samples prepared in Milli-Q water were cut into two semicircular pieces. They became integrated after only 20 min contact at 37°C. The merged piece could be then taken off and support its own weight (Fig. 7d).

In a third approach, one transparent hydrogel and another one containing red Rhodamine B dye prepared in pH 7 buffer were crushed via injection onto a Petri dish using a syringe, and became integrated 20 min later (Fig. 7e). Almost the whole hydrogel was dyed red after 24 h. Similar phenomena were observed in a fourth approach for transparent and dyed red hydrogels prepared in pH 8 buffer (Fig. 7f), demonstrating that the color exchange may be observed via diffusion at the restored self-healed interfaces between different dynagels at pH 7 or pH 8.

These tests strongly demonstrate the outstanding self-healing properties of the dynamic hydrogels - dynagels via reconstruction of reversible imine bond crosslinking, and migration of components or constituent exchanges between different hydrogels. Importantly, the use of these hydrogels with distinct and interchangeable states at different pH conditions would be advantageous for biomedical applications such as drug delivery and tissue engineering.

**3.6 Cytocompatibility of hydrogels:** Human mesenchymal stromal cells (MSCs) isolated from subcutaneous adipose tissue (AT-MSCs) or from bone-marrow (BM-MSCs) were encapsulated inside Gel4-1 ( $1 \times 10^6$  cells/mL), and cultured up to 7 days in proliferative medium at 37 °C to evaluate the cytocompatibility. Compared to control conditions in 2D on TCPS plate or encapsulated in a type I collagen hydrogel, AT-MSCs and BM-MSCs exhibited a round shape in Gel4-1 and not a fibroblastic phenotype (Fig. 8). One day after inclusion in the hydrogel, the large majority of AT-MSCs (95%) and BM-MSCs (99%) were alive as indicated by the green



color in confocal microscopy using live/dead assay, whereas only 66% of viability was observed in type I collagen hydrogel (Fig. 8). The two cell types survived for at least 7 days, as only 1 and 4% of dead cells were quantified for AT-MSCs and BM-MSCs, respectively (Fig. 8). These findings demonstrate the excellent cytocompatibility of the hydrogel. It is noteworthy that the size of AT-MSCs and BM-MSCs after 7 days was smaller than that at day 1, suggesting that the pore size was reduced without affecting cell viability. Three-D reconstruction clearly shows the homogeneous distribution of MSCs in the whole hydrogel volume, indicating that the gelation time was compatible with homogenous distribution of the cells without sedimentation (Vid. S7, Supporting Information).

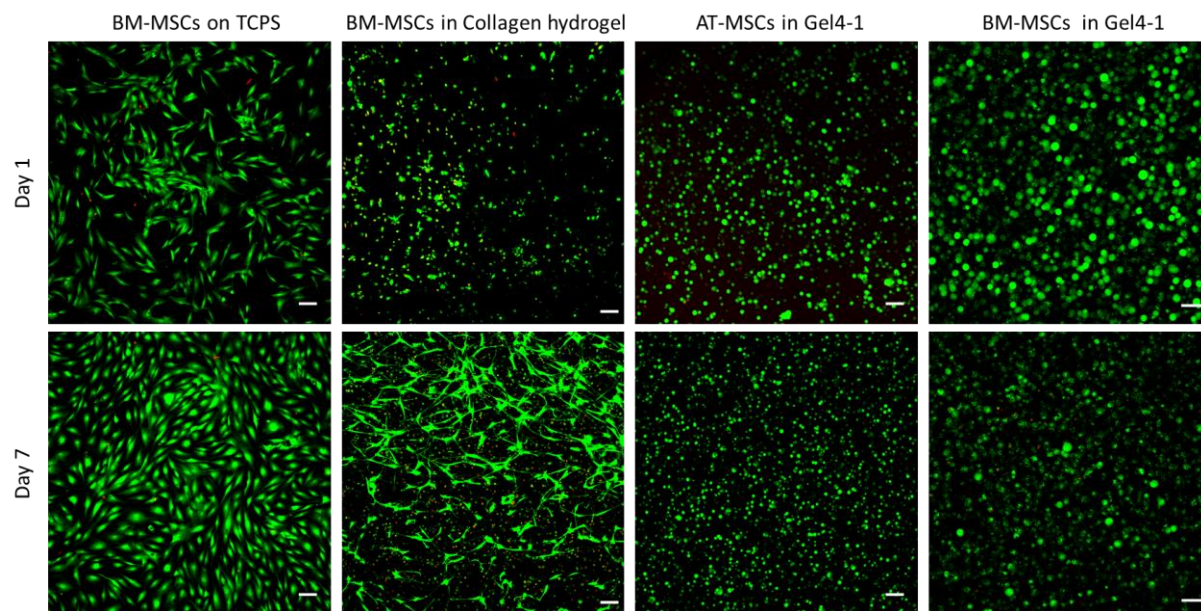


**Fig. 8.** Cell viability of human AT-MSCs or BM-MSCs in Gel4-1, in comparison with BM-MSCs in collagen hydrogel or plated on TCPS as control. Cells were labelled using the Live/Dead assay after 1 or 7 days in culture and imaged using confocal microscopy. Viable cells were stained in green and dead cells in red. Images are maximal projections of z-axis and scale



bars represent 100  $\mu\text{m}$  (TCPS: Tissue Culture Polystyrene Surface; AT-MSCs: Adipose Tissue-MSCs; BM-MSCs: Bone Marrow-MSCs).

#### 4. Conclusions

Multistate pH-sensitive hydrogels were synthesized via dynamic covalent imine bonding from two water soluble polymers, *i.e.* O-carboxymethyl chitosan (CMCS) and a cross-linking dynamer obtained by reaction of amine terminated Jeffamine as connector and Benzene-1,3,5-tricarbaldehyde as core center. The hydrogel Gel4-1 with D-glucosamine to dynamer molar ratio of 4:1 exhibits the shortest gelation time and the highest storage modulus, in agreement with optimal cross-linking or imine bond formation. Freeze-dried gels exhibit interconnected porous structures and pH-dependent swelling behavior. The swelling ratio is relatively low at acidic pH 3-5 due to electrostatic attraction, while became very high, up to 7000 % at pH 8 due to electrostatic repulsion. Moreover, hydrogels present outstanding self-healing properties as evidenced by closure of split pieces and rheological studies. Self-healing occurs autonomously for different pH-dependent states, being able to reshape or to regenerate a strong chemical gel from various situations. Last but not least, MSCs encapsulated in hydrogels are all alive after 7 days, in agreement with the excellent cytocompatibility of hydrogels.

This concept, exploiting different physical swelling states depending on pH values, results in the definition of stimuli-responsive dynagels which self-adapt their structure in response to environmental conditions. These ‘two-in-one’ dynagels may find potential uses in biomedical applications in particular as scaffold in tissue engineering.

#### ASSOCIATED CONTENT

## Supporting Information.

The following files are available free of charge.

NMR spectra of daynamers; rheology data of as-prepared hydrogels; SEM images of freeze dried as-prepared hydrogels and hydrogels after swelling in buffers (pH4, pH8); rheology data of self-healing hydrogels made in buffers (pH7, pH8), 3-D reconstruction of MSCs after 7 days culture in Gel4-1 (AVI).

## ABBREVIATIONS

CMCS, O-carboxymethyl chitosan; Dy, Dynamer; BTA, Benzene-1,3,5-tricarbaldehyde; PBS, phosphate buffered saline; TMS, tetramethylsilane; MSCs, human mesenchymal stromal cells.

## ACKNOWLEDGMENT

This work is supported by the scholarship from China Scholarship Council (CSC) under the Grant CSC N° 201706240281, and the Institut Européen des Membranes (Exploratory project “Biostent - Health” of the Internal IEM Call 2017). Authors acknowledge funding support from the Inserm Institute and the University of Montpellier.

## REFERENCES

- Ali, A., & Ahmed, S. (2018). A review on chitosan and its nanocomposites in drug delivery. *International Journal of Biological Macromolecules*, 109, 273-286.
- Arnal-Hérault, C., Banu, A., Barboiu, M., Michau, M., & van der Lee, A. (2007). Amplification and transcription of the dynamic supramolecular chirality of the guanine quadruplex. *Angewandte Chemie International Edition*, 46(23), 4268-4272.
- Bhatia, S. K. (2010). Traumatic injuries. In *Biomaterials for clinical applications* (pp. 213-258): Springer
- Burdick, J. A., & Murphy, W. L. (2012). Moving from static to dynamic complexity in hydrogel design. *Nature Communications*, 3(1), 1-8.

- Catana, R., Barboiu, M., Moleavin, I., Clima, L., Rotaru, A., Ursu, E.-L., & Pinteala, M. (2015). Dynamic constitutional frameworks for DNA biomimetic recognition. *Chemical Communications*, 51(11), 2021-2024.
- Chao, A., Negulescu, I., & Zhang, D. (2016). Dynamic covalent polymer networks based on degenerative imine bond exchange: tuning the malleability and self-healing properties by solvent. *Macromolecules*, 49(17), 6277-6284.
- Deng, G., Ma, Q., Yu, H., Zhang, Y., Yan, Z., Liu, F., et al. (2015). Macroscopic organohydrogel hybrid from rapid adhesion between dynamic covalent hydrogel and organogel. *ACS Macro Letters*, 4(4), 467-471.
- Dimatteo, R., Darling, N. J., & Segura, T. (2018). In situ forming injectable hydrogels for drug delivery and wound repair. *Advanced Drug Delivery Reviews*, 127, 167-184.
- Ghobril, C., & Grinstaff, M. (2015). The chemistry and engineering of polymeric hydrogel adhesives for wound closure: a tutorial. *Chemical Society Reviews*, 44(7), 1820-1835.
- Huang, W., Wang, Y., Chen, Y., Zhao, Y., Zhang, Q., Zheng, X., et al. (2016). Strong and rapidly self-Healing hydrogels: potential hemostatic materials. *Advanced Healthcare Materials*, 5(21), 2813-2822.
- Iftime, M. M., Morariu, S., & Marin, L. (2017). Salicyl-imine-chitosan hydrogels: Supramolecular architecturing as a crosslinking method toward multifunctional hydrogels. *Carbohydrate Polymers*, 165, 39-50.
- Li, S., El Ghzaoui, A., & Dewinck, E. (2005). Rheology and drug release properties of bioresorbable hydrogels prepared from polylactide/poly (ethylene glycol) block copolymers. *Macromolecular Symposia* (Vol. 222, pp. 23-36): Wiley Online Library.
- Lv, X., Zhang, W., Liu, Y., Zhao, Y., Zhang, J., & Hou, M. (2018). Hygroscopicity modulation of hydrogels based on carboxymethyl chitosan/Alginate polyelectrolyte complexes and its application as pH-sensitive delivery system. *Carbohydrate Polymers*, 198, 86-93.
- Marin, L., Moraru, S., Popescu, M. C., Nicolescu, A., Zgardan, C., Simionescu, B. C., et al. (2014). Out-of-water constitutional self-organization of chitosan-cinnamaldehyde dynagels. *Chemistry-A European Journal*, 20(16), 4814-4821.
- Marin, L., Simionescu, B., & Barboiu, M. (2012). Imino-chitosan biodynamers. *Chemical Communications*, 48(70), 8778-8780.
- Qiao, C., Ma, X., Zhang, J., & Yao, J. (2017). Molecular interactions in gelatin/chitosan composite films. *Food Chemistry*, 235, 45-50.
- Qin, C., Zhou, J., Zhang, Z., Chen, W., Hu, Q., & Wang, Y. (2019). Convenient one-step approach based on stimuli-responsive sol-gel transition properties to directly build chitosan-alginate core-shell beads. *Food Hydrocolloids*, 87, 253-259.
- Qu, J., Zhao, X., Liang, Y., Zhang, T., Ma, P. X., & Guo, B. (2018). Antibacterial adhesive injectable hydrogels with rapid self-healing, extensibility and compressibility as wound dressing for joints skin wound healing. *Biomaterials*, 183, 185-199.
- Rotaru, A., Pricope, G., Plank, T. N., Clima, L., Ursu, E. L., Pinteala, M., et al. (2017). G-Quartet hydrogels for effective cell growth applications. *Chemical Communications*, 53(94), 12668-12671.
- Sreenivasachary, N., & Lehn, J.-M. (2005). Gelation-driven component selection in the generation of constitutional dynamic hydrogels based on guanine-quartet formation. *Proceedings of the National Academy of Sciences of the United States of America*, 102(17), 5938-5943.

- Stewart, D., Antypov, D., Dyer, M. S., Pitcher, M. J., Katsoulidis, A. P., Chater, P. A., et al. (2017). Stable and ordered amide frameworks synthesised under reversible conditions which facilitate error checking. *Nature Communications*, 8(1), 1102.
- Su, F., Wang, J., Zhu, S., Liu, S., Yu, X., & Li, S. (2015). Synthesis and characterization of novel carboxymethyl chitosan grafted polylactide hydrogels for controlled drug delivery. *Polymers for Advanced Technologies*, 26(8), 924-931.
- Van Vlierberghe, S., Dubruel, P., & Schacht, E. (2011). Biopolymer-based hydrogels as scaffolds for tissue engineering applications: a review. *Biomacromolecules*, 12(5), 1387-1408.
- Varum, K. M., Ottoy, M. H., & Smidsrod, O. (1994). Water-solubility of partially N-acetylated chitosans as a function of pH: effect of chemical composition and depolymerisation. *Carbohydrate Polymers*, 25(2), 65-70.
- Yang, Y., Wang, X., Yang, F., Wang, L., & Wu, D. (2018). Highly elastic and ultratough hybrid ionic-covalent hydrogels with tunable structures and mechanics. *Advanced Materials*, 30(18), 1707071.
- Yu, S., Zhang, X., Tan, G., Tian, L., Liu, D., Liu, Y., et al. (2017). A novel pH-induced thermosensitive hydrogel composed of carboxymethyl chitosan and poloxamer cross-linked by glutaraldehyde for ophthalmic drug delivery. *Carbohydrate Polymers*, 155, 208-217.
- Zeng, X., Liu, G., Tao, W., Ma, Y., Zhang, X., He, F., et al. (2017). A drug-self-gated mesoporous antitumor nanoplatfrom based on pH-sensitive dynamic covalent bond. *Advanced Functional Materials*, 27(11), 1605985.
- Zhang, W., Jin, X., Li, H., Zhang, R., & Wu, C. (2018). Injectable and body temperature sensitive hydrogels based on chitosan and hyaluronic acid for pH sensitive drug release. *Carbohydrate Polymers*, 186, 82-90.
- Zhang, Y., & Barboiu, M. (2015a). Dynameric asymmetric membranes for directional water transport. *Chemical Communications*, 51(88), 15925-15927.
- Zhang, Y., & Barboiu, M. (2015b). Constitutional dynamic materials toward natural selection of function. *Chemical Reviews*, 116(3), 809-834.
- Zhang, Y., Tao, L., Li, S., & Wei, Y. (2011). Synthesis of multiresponsive and dynamic chitosan-based hydrogels for controlled release of bioactive molecules. *Biomacromolecules*, 12(8), 2894-2901.
- Zhang, Y., Wu, X., Han, Y., Mo, F., Duan, Y., & Li, S. (2010). Novel thymopentin release systems prepared from bioresorbable PLA-PEG-PLA hydrogels. *International Journal of Pharmaceutics*, 386(1-2), 15-22.
- Zimmermann, J., Bittner, K., Stark, B., & Mülhaupt, R. (2002). Novel hydrogels as supports for in vitro cell growth: poly (ethylene glycol) and gelatin-based (meth) acrylamido peptide macromonomers. *Biomaterials*, 23(10), 2127-2134.